



## RESEARCH ARTICLE

**The kinetics of the oxidation of ammonia on a  $V_2O_5/TiO_2$  SCR catalyst deactivated in an engine rig. Part I. Determination of kinetic parameters by simulation**Ingemar Odenbrand<sup>1</sup> <sup>1</sup>Department of Chemical Engineering, Lund University, P.O. Box 124, SE-221 00 Lund, SWEDEN

## ABSTRACT

It is shown how the deactivation of a diesel SCR (Selective Catalytic Reduction) catalyst by compounds in the exhaust gases influences the kinetics of the catalyst. Results are given for the fresh (4.56 %  $V_2O_5/TiO_2$ ) catalyst and the ones used in the rig for 890 h and 2299 h. The reactions of 700 ppm  $NH_3$  and 2 %  $O_2$  in Helium yielded  $N_2$ ,  $N_2O$ , and  $NO$  at increasing temperatures. Simulations were performed with COMSOL Multiphysics using a 3-D model of the catalyst system. The experimental values of the products  $N_2$ ,  $N_2O$ , and  $NO$  were very nicely fitted by the kinetic model used. All three ammonia oxidation reaction rates were of the first order in the concentration of  $NH_3$ . A preliminary study using non-isothermal conditions showed the maximal temperature increase to be 0.15 K. Thus, further simulations were done with an isothermal model. The deactivation reduces the pre-exponential factors and the activation energies for the formation of  $N_2$ ,  $N_2O$ , and  $NO$ . The formation of  $N_2$  is not substantially influenced by deactivation. The changes in the kinetics of the catalytic  $NH_3$  oxidation by deactivation is reported for the first time in the present study.

**Keywords:** Oxidation of ammonia, poisoning and kinetics, Vanadia SCR diesel catalysts

## 1. INTRODUCTION

The Selective Catalytic Reduction (SCR) technique is today a compulsory method for mobile applications like marine and automotive diesel engines in many countries. Marine engines run under conditions, which resemble the ones in stationary diesel power plants. In 2017, there were hundreds of SCR units installed on diesel engines on ships [1]. The lubricating oil for the diesel engine is often a source for deactivation components for the catalyst. A SAE 15W-40 oil contained 0.26, 0.25, 0.068, and 0.061 wt. % of S, Ca, Zn, and P, respectively [2]. These components will influence the performance of the SCR catalyst, as shown in a previous publication [3]. In that study, it was shown how the activity and selectivity in the SCR system are influenced by poisoning. It is interesting to elucidate the role of ammonia oxidation reactions in the SCR system. They do contribute to unwarranted  $N_2O$  production and the destruction of  $NH_3$  at the high temperatures sometimes reached in diesel applications. Koebel and Elsener [4] studied the removal of 1000 ppm  $NO$  with  $NH_3$  using commercial  $V_2O_5-WO_3-TiO_2$  catalysts. They do not state what

ammonia reaction(s) they consider but state that the rates of ammonia oxidation reactions are about 500 times smaller than the SCR reaction ones. In 1993 Ozkan et al. [5] studied the role of ammonia oxidation in the SCR over vanadia catalysts. They found that  $N_2$ ,  $N_2O$ , and  $NO$  were the products. In their extensive study [6] using nitrogen labelling, they found that the ammonia species giving  $N_2$  and  $N_2O$  have relative long residence times on the surface. The  $NO$  producing species are short-lived. Thus, three ammonia oxidation reactions are assumed. Duffy et al. [7], using  $V_2O_5/TiO_2$  catalysts with varying vanadia contents, also used isotopic labelling studies to conclude that below 300 °C  $^{14}N^{15}N$  is always the major product from  $^{15}NO$  and  $^{14}NH_3$ . At higher temperatures, the product distribution is susceptible to the vanadia content of the catalyst. At 500 °C, 70 % of the product is  $^{14}NO$ . Pure  $V_2O_5$  produces significantly more  $^{14}N^{15}NO$ , and at lower temperatures than a 1.4 wt %  $V_2O_5/TiO_2$  catalyst. As part of an SCR study, the kinetics of the partial ammonia oxidation giving  $N_2$  was studied between 250 and 300 °C by Efstathiou et al. [8]. They oxidised 1000 ppm  $NH_3$  by 2 %  $O_2$  with helium as background gas over an 8 mol %  $V_2O_5/TiO_2$  catalyst. The selectivity to

Corresponding Author: [ingemar.odenbrand@chemeng.lth.se](mailto:ingemar.odenbrand@chemeng.lth.se) (C.U. Ingemar Odenbrand)

Received 29 June 2019; Received in revised form 11 December 2019; Accepted 12 December 2019

Available Online: 14 December 2019

Doi: <https://doi.org/10.35208/ert.597731>

© Yildiz Technical University, Environmental Engineering Department. All rights reserved.

N<sub>2</sub> was from 98.2 to 97.6 % decreasing with temperature. The rate of the ammonia oxidation was only from 1.8 to 2.4 % of the rate of the SCR reaction, much higher than stated above by Koebel and Elsener [4]. They [8] also studied the formation of N<sub>2</sub>O between 320 and 380 °C. In this temperature range, the formation of N<sub>2</sub>O is almost completely caused by the reaction of NH<sub>3</sub> with NO. Djerad et al. [9] included all three NH<sub>3</sub> oxidation reactions in their study on the effect of oxygen on the reaction rates. Using a 3%V, 9%W on titania catalysts, the effect of oxygen was small between 2 and 15 % O<sub>2</sub>. A maximum in the formation of N<sub>2</sub> was observed at 425 °C, N<sub>2</sub>O was formed above 300 °C while NO only above 425 °C. They found that the formation of N<sub>2</sub>O from ammonia oxidation is important in the SCR process. So, we will include all three reactions in our simulation of the ammonia oxidation.

The inspiration for the present study comes from the excellent results obtained earlier using COMSOL Multiphysics as means of performing FEM analysis of catalytic reactors [10,11]. An excellent paper on global kinetic modelling of SCR over vanadia on titania was published by Roduit et al. [12]. Only the SCR reaction and the oxidation of NH<sub>3</sub> to N<sub>2</sub> were included though. They presented results on the ammonia coverage of the catalyst as a function of temperature and ammonia concentration. These values were the base for our assumed influence of temperature on the coverage of NH<sub>3</sub>. Their values of the adsorption energy of NH<sub>3</sub> was not used. Instead, we relied on the value -100 to -130 kJ mol<sup>-1</sup>, as presented by Koebel and Elsener [4].

There are not too many studies published using COMSOL Multiphysics to simulate catalytic reactors. One of them is performed by Chen et al. [13]. They used their study to optimise the performance of the reactor for the SCR using the NH<sub>3</sub> to N<sub>2</sub> oxidation reaction and the SCR reaction.

We could not find very much if any, kind of information in the literature on the effect of deactivation on the kinetics of ammonia oxidation over vanadia catalysts. We presented before [3] how the poisons accumulate along the catalyst monolith. The present study presents a simulation of the kinetics of the oxidation of NH<sub>3</sub> with O<sub>2</sub> and how it depends on the degree of the poisoning of the catalyst. The catalysts in this study consist of a thin layer of active components supported on cordierite. Therefore, the effect of deactivation will be more easily detected in our experiments than in experiments on full catalysts.

The data used in the study were measured at two increasing degrees of poisoning by the compounds most likely to be present in commercial use. Therefore, the result could be used in the design of new catalysts for diesel engines which are deactivated by compounds in the lubrication oil.

## 2. MATERIALS AND METHODS

### 2.1. Preparation and deactivation of the catalyst samples

The catalysts used were made in house by a Swedish catalyst manufacturer and consisted of 5.64 % V<sub>2</sub>O<sub>5</sub> on

TiO<sub>2</sub> (Rhone Poulenc DT(8)) on the support of cordierite from Corning with a CPSI of 400. Details on the preparation, deactivation and characterisation can be found in Odenbrand [3]. The deactivation was performed in an engine rig using Swedish class 1 diesel fuel. The deactivation cycle, 1 hour long, had a mean temperature of 470 °C and a maximum temperature of 570 °C for 7.5 min in each cycle. Samples were taken from the fresh catalyst, and the catalysts used for 890 and 2299 h in the rig. The accelerated test was supposed to simulate the regular running of a truck for up to 500 000 km (given by the catalyst manufacturer).

### 2.2. Measurement of catalyst activity and selectivity

The centre part (9 x 9 channels wide) of the 10 cm long and 2.5 cm wide monolithic catalysts were cut into 1 cm mini monoliths along their axis. Only piece five from the inlet was used in the ammonia oxidation experiments. The activity and selectivity in the oxidation of ammonia with O<sub>2</sub> were measured at about 700 ppm NH<sub>3</sub> and 2 % O<sub>2</sub>. The pressure was 1.24 bar (Space velocity 45 000 h<sup>-1</sup>). Temperatures were from 340 to 460 °C at 20 °C intervals. Helium was used as a background gas containing about 3000 ppm of Ar for internal calibration as described before [11]. A Balzer QMG 311 mass spectrometer was used for gas analysis. A chopping device was used to decrease the influence of the background signal. The spectra were recorded using peaks 17, 18, 28, 30, 34, 40, 44 and 46 for NH<sub>3</sub>, H<sub>2</sub>O, N<sub>2</sub>, NO, O<sub>2</sub>, Ar, N<sub>2</sub>O and NO<sub>2</sub>. The spectrum was scanned twice first with an open and then with a closed chopper. By subtraction, a difference spectrum representing the composition in the gas stream was obtained. Experimentally determined splitting factors and sensitivity factors, determined from gases of known compositions, were used to calculate the concentrations with a computer program. The background concentrations of N<sub>2</sub> and H<sub>2</sub>O were 37.7 ± 0.2 and 31.4 ± 2.5 ppm respectively showing the accuracy of the mass spectrometric data. Inlet concentrations of NH<sub>3</sub> varied somewhat between the three experiments and were 725 ± 18 ppm. The actual concentrations were used in the simulation of each series of experiments.

### 2.3. Modelling of the catalyst reactions

The kinetic scheme used in the simulations is based on first-order reactions in the concentration of ammonia for reactions 2, 4 and 5 in Table 1. In all cases, the effect of oxygen, present in excess (2 %), is included in the rate constant. The eventual effects of any diffusion limitations are also included.

The reactions are demanding more and more oxygen and are being more important at increased temperatures, the higher the number of the reaction is. It is only reactions 2, 4 and 5 that have a significant influence on the kinetics of ammonia oxidation because of deficient concentrations of NO in the system. Thus, reactions 1 and 3 are omitted in this study. Table 2 shows the physiochemical data used in the simulation in non-isothermal and in isothermal cases.

**Table 1.** Chemical reactions and kinetic expressions used in the simulations

Reaction number	Global reaction	Rate expression
1	$4\text{NH}_3+4\text{NO}+\text{O}_2\Rightarrow 4\text{N}_2+6\text{H}_2\text{O}$	$r_1 = A_1 \cdot \exp(-E_1/(R \cdot T)) \cdot c_{\text{NO}} \cdot \theta_{\text{NH}_3}$
2	$4\text{NH}_3+3\text{O}_2\Rightarrow 2\text{N}_2+6\text{H}_2\text{O}$	$r_2 = A_2 \cdot \exp(-E_1/(R \cdot T)) \cdot c_{\text{NH}_3}$
3	$4\text{NH}_3+4\text{NO}+\text{O}_2\Rightarrow 4\text{N}_2\text{O}+6\text{H}_2\text{O}$	$r_3 = A_3 \cdot \exp(-E_1/(R \cdot T)) \cdot c_{\text{NO}} \cdot \theta_{\text{NH}_3}$
4	$4\text{NH}_3+4\text{O}_2\Rightarrow 2\text{N}_2\text{O}+6\text{H}_2\text{O}$	$r_4 = A_4 \cdot \exp(-E_1/(R \cdot T)) \cdot c_{\text{NH}_3}$
5	$4\text{NH}_3+5\text{O}_2\Rightarrow 4\text{NO}+6\text{H}_2\text{O}$	$r_5 = A_5 \cdot \exp(-E_1/(R \cdot T)) \cdot c_{\text{NH}_3}$

$$\theta_{\text{NH}_3} = K_{\text{NH}_3} \cdot c_{\text{NH}_3} / (1 + K_{\text{NH}_3} \cdot c_{\text{NH}_3}), K_{\text{NH}_3} = A_0 \cdot \exp(-E_0/(R \cdot T))$$

**Table 2.** Physical data used in the Transport of Diluted Species and Free and Porous Media Flow nodes in the COMSOL program

Parameter	Open channel	Catalyst Layer	Cordierite <sup>1</sup>
Diffusion coefficients in the fluid *10 <sup>5</sup> (m <sup>2</sup> s <sup>-1</sup> )	9.83 - 13.22	n.a.	n.a.
Diffusion coefficients in catalyst (m <sup>2</sup> s <sup>-1</sup> )	n.a.	Deff=ε/τ*Dfluid τ = ε-(1/3)	n.a.
Porosity of catalyst (ε)	n.a.	0.4	n.a.
Density (kg m <sup>-3</sup> )	0.635 - 0.760	2295	2300
Dynamic viscosity *10 <sup>5</sup> (Pas)	9.25 - 10.39	n.a.	n.a.
Permeability (m <sup>2</sup> )	n.a.	6*10-8 [11]	n.a.
Thermal conductivity (W (m <sup>-1</sup> K <sup>-1</sup> ))	0.090 - 0.101	8.4	1.8
Heat capacity (J (kg <sup>-1</sup> K <sup>-1</sup> ))	649	1050	880
The ratio of specific heats	1	1	1

n.a. Not applicable

1) Cordierite was substituted by concrete, and alumina was used instead of titania for physical data

The heat source was from the chemical reactions. The system is mostly calculated isothermally. Therefore, the properties of the cordierite are not included in the major part of the simulations. Incompressible flow with a normal inlet velocity of  $v_{in}$  in the direction of the reactor axis was used for the Free and Porous Media Flow node. The total flow ( $Q_{in}$ ) at NTP was 0.9 l min<sup>-1</sup>. It was distributed over 9\*9 square channels and was  $1.8519 \cdot 10^{-7}$  m<sup>3</sup> s<sup>-1</sup> at NTP for one channel. The inlet open surface area of one channel was  $2.1316 \cdot 10^{-6}$  m<sup>2</sup>. The reference pressure (pref) was 1 bar, and the total one (ptot) was 1.236 bar. Thus,  $v_{in} = Q_{in}/A_{in} \cdot T_{in}/273.15/ptot \cdot pref$  (0.157 m s<sup>-1</sup> at 613 K (340 °C)). The program calculates the varying velocities at different temperatures.

The densities for V<sub>2</sub>O<sub>5</sub> is 4571 and for TiO<sub>2</sub> 3780 kg m<sup>-3</sup>. Then the solid density of the active catalyst layer is thus  $0.0564 \cdot 4571 + (1-0.0564) \cdot 3780$  yielding a solid density of 3825 kg m<sup>-3</sup> for the catalyst layer containing 5.64 % V<sub>2</sub>O<sub>5</sub>. The porosity is 0.4 as measured before, and so the apparent density is 2295 kg m<sup>-3</sup>. The apparent density, together with the amount of the active phase (18.2 wt %), is used in calculating the thickness of the active layer to 21 μm, which was used in the simulations. The catalyst layer was supposed to cover all inside walls of the monolith. For calculation speed reasons only one-eighth of the whole reactor was simulated. The mesh used is shown in Fig 1.



**Fig 1.** Reactor model, showing the mesh, used in the simulations (1/8 of the whole model). The gas inlet is from the left. The mini monolith is 1 cm long and has a 21 μm catalyst layer on all walls

The reactor, made of quartz glass, is 100 mm long with the bottom of the catalyst monolith (1 cm long) positioned 60 mm from the inlet on a plug of glass wool. The monolith was surrounded by quartz wool to stop gas bypassing the catalyst. Only a small part of the simulated system is shown (Fig 2) in order to show the mesh used in the calculations. The monolith contains 81 channels, but the model simulates only one of them.

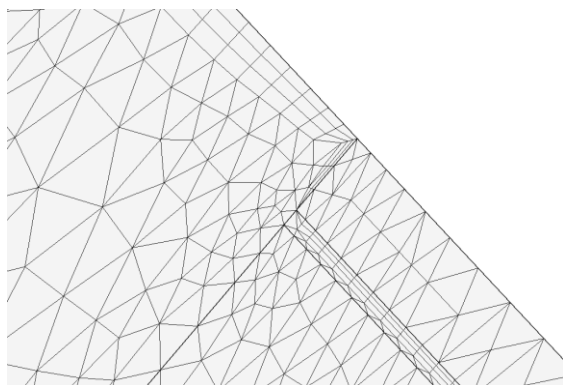


**Fig 2.** Enlargement of the inlet section of the monolith part of the reactor model, showing the mesh, used in the simulations (1/8 of the whole model). Boundary layers are present both in the open channel and along with the catalyst layer. The gas inlet is from the left. The mini monolith is 1 cm long and has a 21  $\mu\text{m}$  catalyst layer on all walls

COMSOL Multiphysics ver. 5.4 was used in the simulations in a similar way as described before [10, 11] with the data given in Table 2. The reactor was placed in a heated chamber with forced circulation of the air. Heat flux was used as the boundary condition on the outside of the reactor walls for the non-isothermal cases. The heat was transferred by convection from the reactor outside to the air flowing over its outside, according to  $q_0 = h \cdot (T_{\text{in}} - T)$ . The value for  $h$  was 100  $\text{W}/\text{m}^2/\text{K}$  taken from [14] for forced convection, medium speed flow of air over a surface. The physic-controlled mesh was used with a coarse element size. The degrees of freedom (DOF) for the non-isothermal case was 2 335 934 plus 195 579 internal degrees of freedom (DOF). For the isothermal one, it was 492 990 plus 165 510 internal degrees of

**Table 3.** Inlet concentrations (ppm) used in the simulations of the oxidation of  $\text{NH}_3$  for the three catalysts studied

Catalyst	$\text{NH}_3$	$\text{N}_2\text{O}$	$\text{NO}$	$\text{N}_2$	$\text{H}_2\text{O}$
Fresh	728.8	1.2	4.6	37.4	28.2
890 h	745.6	1.0	3.8	37.8	31.6
2299 h	702.0	2.0	4.0	37.8	34.4

Concentrations measured at the end of the reactor were shown by the simulations to be even over the channel cross-section. The measured concentrations are plotted versus the temperature at the exit of the monolith. Manual changes in kinetic parameters are performed in order to fit the simulated values to the experimental ones according to the method described before [11, 12]. First, the concentration of  $\text{N}_2$  was fitted with parameters in reaction 2. Then the concentrations of  $\text{N}_2\text{O}$  and  $\text{NO}$  were fitted according to reactions 4 and 5. Both these components were of the same magnitude, so they were fitted simultaneously

### 3. RESULTS AND DISCUSSION

#### 3.1. Apparent kinetic data

Table 4 shows apparent kinetic data which were obtained from assumed first-order dependence on the concentration of  $\text{NH}_3$  and experimental conversions

freedom. When the physics-controlled mesh is used, three boundary layers close to the walls were introduced to get a fine resolution of the velocity profile in that position. The solution for the non-isothermal case was obtained by performing two separate stationary studies. Study one was performed in 3 steps. The Free and Porous Media Flow node was calculated in step 1 at 773 K. In step 2, the following nodes were used Chemistry, Transport of Diluted Species, and Heat Transfer in Porous Media. Finally, in step 3, all above nodes were used plus the Domain ODEs and DAEs used for calculation of the temperature dependence of the heat of adsorption of ammonia. In the stationary study two, all nodes were used, and initial values of variables were taken from study one step three. The temperature was decreased from 733 K downwards to 613 in steps of 20 K for easier convergence. The solver was PARDISO and the variables  $u$  and  $p$  were solved in segregated step one, the temperature in step two, all concentrations in step three, and the heat of adsorption of ammonia ( $E_0$ ) in step four. The isothermal case contained fewer steps and only reactions 2, 4 and 5.

The details of the simulation equations and boundary and subdomain settings are the same as in reference [11].

#### 2.4. Inlet concentrations for the simulation of ammonia oxidation

Table 3 shows the inlet data used in the simulations of the oxidation of  $\text{NH}_3$  with 2 %  $\text{O}_2$  for the three catalysts studied. The fitted concentrations are  $\text{N}_2$ ,  $\text{N}_2\text{O}$  and  $\text{NO}$ . The others are the result of the reaction stoichiometry.

and selectivities. These parameters were used as starting values in the simulations.

Rates are given at 340 and 460  $^\circ\text{C}$  except for  $r_{\text{NO}}$  for the fresh catalyst and the one used for 890 h where the lowest temperature is 380  $^\circ\text{C}$ .

The activation energies are decreasing with an increased degree of poisoning, as observed before [15, 16]. The poisoning has the most significant effect on the formation of  $\text{NO}$ . The results of this study can be compared to the results of Chen and Tan [13] who also used COMSOL Multiphysics in the simulation of, in their case, a catalyst bed. Their value of  $E_2$  is 84.4  $\text{kJ mol}^{-1}$  when corrected for diffusion limitations while our apparent value is 74.4  $\text{kJ mol}^{-1}$  for the fresh catalyst. The values of  $k_2$  were  $6.73 \cdot 10^7$  and  $4.13 \cdot 10^8 \text{ s}^{-1}$ , respectively. Good consistency is obtained.

**Table 4.** Apparent kinetic parameters in the oxidation of 700 ppm NH<sub>3</sub> with 2 % O<sub>2</sub> in Helium at 1.24 atm from 340 to 460 °C on all three catalysts

Parameter	Fresh	890 h	2299 h
A <sub>2</sub> (m <sup>3</sup> g <sup>-1</sup> s <sup>-1</sup> )	9.79*10 <sup>5</sup>	9.79*10 <sup>5</sup>	8.95*10 <sup>4</sup>
E <sub>2</sub> (kJ mol <sup>-1</sup> )	74	78	52
r <sub>N<sub>2</sub></sub> (mol g <sup>-1</sup> s <sup>-1</sup> )	4.27*10 <sup>-8</sup> -4.27*10 <sup>-7</sup>	4.27*10 <sup>-8</sup> -4.12*10 <sup>-7</sup>	4.71*10 <sup>-8</sup> -2.62*10 <sup>-7</sup>
A <sub>4</sub> (m <sup>3</sup> g <sup>-1</sup> s <sup>-1</sup> )	4.51*10 <sup>8</sup>	6.68*10 <sup>9</sup>	5.53*10 <sup>9</sup>
E <sub>4</sub> (kJ mol <sup>-1</sup> )	123	137	123
r <sub>N<sub>2</sub>O</sub> (mol g <sup>-1</sup> s <sup>-1</sup> )	2.51*10 <sup>-9</sup> -1.07*10 <sup>-7</sup>	2.99*10 <sup>-9</sup> -1.88*10 <sup>-7</sup>	1.88*10 <sup>-9</sup> -1.31*10 <sup>-7</sup>
A <sub>5</sub> (m <sup>3</sup> g <sup>-1</sup> s <sup>-1</sup> )	3.94*10 <sup>13</sup>	5.69*10 <sup>10</sup>	4.50*10 <sup>10</sup>
E <sub>5</sub> (kJ mol <sup>-1</sup> )	201	161	141
r <sub>NO</sub> (mol g <sup>-1</sup> s <sup>-1</sup> )	3.54*10 <sup>-10</sup> -1.62*10 <sup>-8</sup>	1.32*10 <sup>-9</sup> -2.34*10 <sup>-8</sup>	7.53*10 <sup>-10</sup> -5.30*10 <sup>-8</sup>

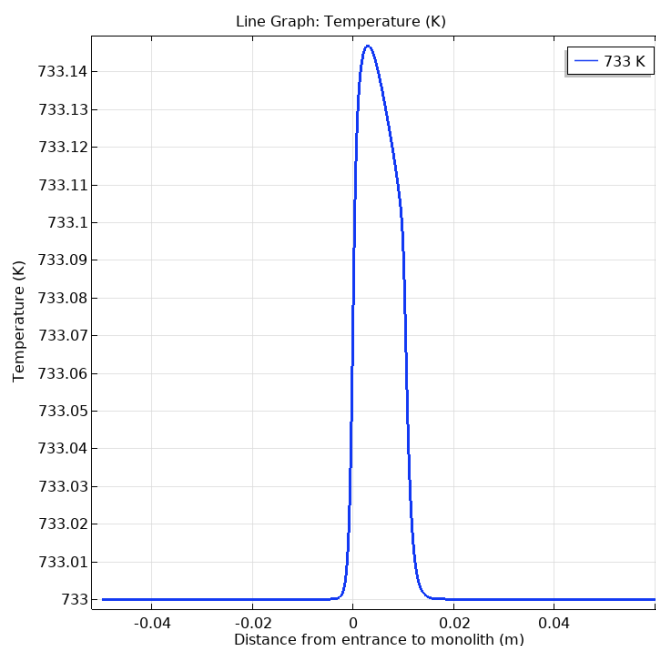
### 3.2. Results from non-isothermal simulations

Fig 3 shows the temperature rise obtained in a non-isothermal simulation. The temperature increase was shown to be only 0.145 °C at 460 °C in the oxidation of 729 ppm NH<sub>3</sub> for the fresh catalyst. The temperature increase is about the same for all three catalysts. These values are small enough so that the assumption of an isothermal system could be used. Even so, the system was simulated as a non-isothermal one first to study some of its properties. One of the most crucial property is the temperature which influences the rate of reactions in an exponential manner

The catalyst monolith starts at 0 and ends at 0.01 m in Fig 3. Increased temperatures are seen both before and after the monolith part of the system caused by heat conduction — the temperature increases along the system axis in a manner typical for exothermal reactions. A maximal temperature is reached at 0.003 m from the inlet of the monolith.

Fig 4 shows how the velocity in the reactor is increased from about 0.39 m s<sup>-1</sup> in the centre before the monolith to about 0.55 m s<sup>-1</sup> inside it. The smaller open channel inside the monolith than in the empty reactor causes this. The flow is developing to a laminar one at about 1 mm from the inlet (not shown here). The pressure drops over the monolith by 5.1\*10<sup>-5</sup> bar and by 3.15\*10<sup>-4</sup> bar over the whole reactor. The total pressure drop over the monolith was only 0.4 % of the actual pressure in the system.

Fig 5 shows how the NH<sub>3</sub> is evenly distributed over the cross-section of the channel, the catalyst layer and the cordierite wall. The lowest value is 545.9 ppm in the centre of the channel, increasing to 550.3 ppm in the upper part of the catalyst layer. That is the concentration is constant within 0.8 % at these conditions. The heat of the reaction is very well distributed over the exit of the monolith, where the maximum temperature difference is only 0.15 K (not shown here). Fig 6 shows the amount of NH<sub>3</sub> “converted” as a function of the position in the monolith and measured in the centre of the channel.

**Fig 3.** The temperature along the axis of the channel around the monolith for the catalyst used for 890 h. Oxidation of 729 ppm NH<sub>3</sub> with 2 % O<sub>2</sub> in Helium. The inlet temperature was 733 K (460 °C).

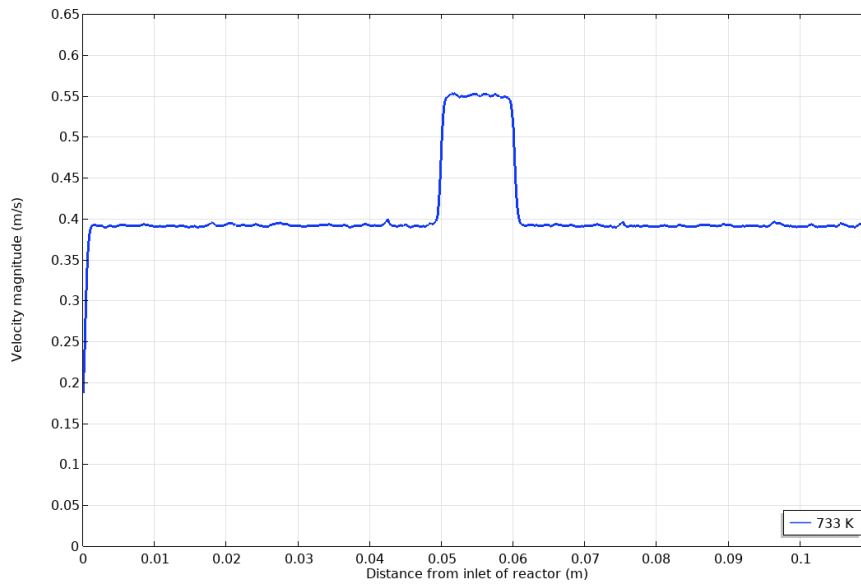


Fig 4. Velocity in the centre of the channel in the reactor. The inlet temperature was 733 K (460 °C), p 1.236 bar

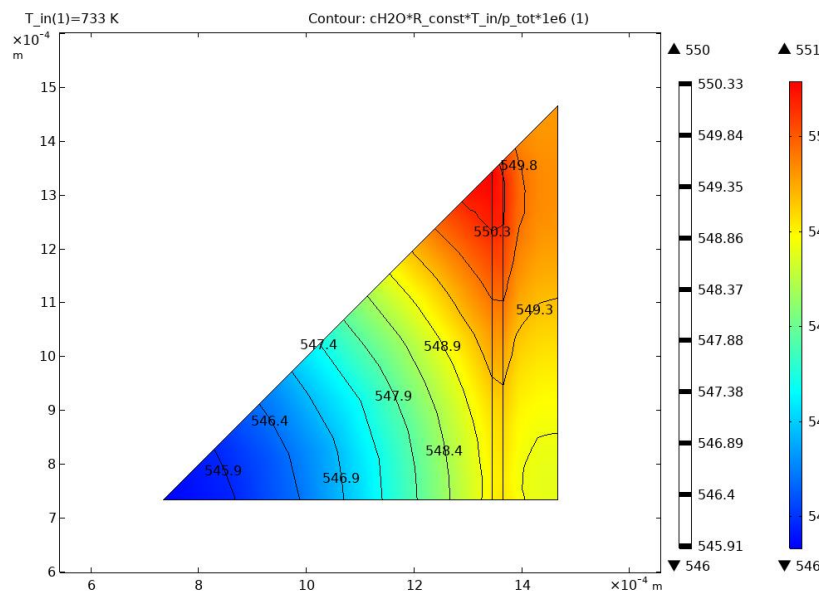


Fig 5. The concentration of NH<sub>3</sub> (ppm) across the surface of the channel, the fresh catalyst layer and the monolith wall at the exit of the monolith. The inlet temperature was 733 K (460 °C)

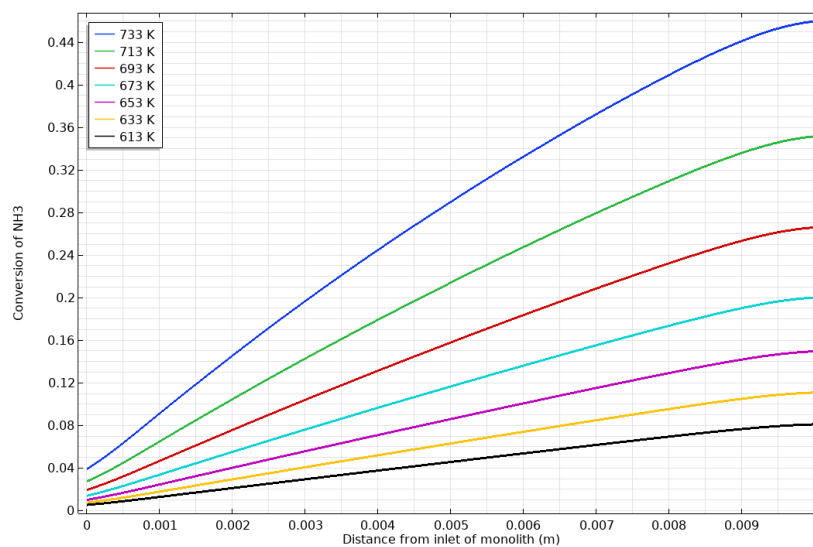


Fig 6. The conversion of NH<sub>3</sub> along the axis of the channel for the fresh monolith. The inlet temperature was 733 K (460 °C)

In the inlet part of the monolith, there is a definite "conversion" caused by a change in concentration as an effect of the increased temperature in this position (Fig 3). One would not expect a conversion before the gas stream is in contact with the catalyst. That is why we use apostrophes around conversion.

The rate of formation of nitrogen is 60 times higher than the rate of formation of nitrous oxide at 340 °C (613 K in Fig 7). At 460 °C the ratio is only 2.26. The rate of formation of NO is even lower and is only 0.39 % of the rate of formation of nitrogen at 340 °C. At 460 °C it increases to 8.6 % of the rate of formation of nitrogen.

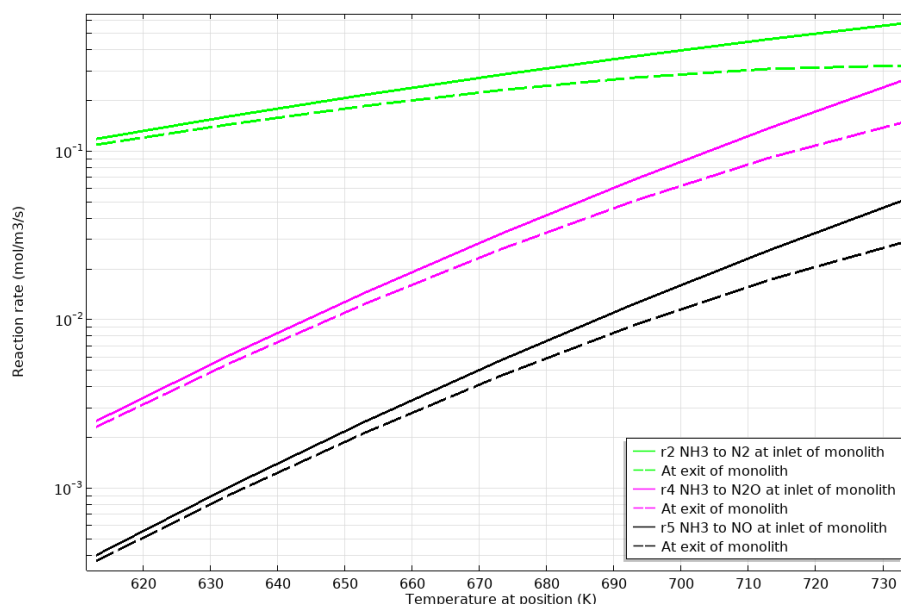


Fig 7. The rates of the individual reactions as a function of the temperature for the fresh catalyst

### 3.3. Results from isothermal simulations

Since the maximal temperature increase is so low, the rest of the simulations were performed as an isothermal case. Fig 8 shows the concentrations of products formed in the oxidation of about 800 ppm NH<sub>3</sub> with 2 % O<sub>2</sub> along with the simulated values for the fresh catalyst, for the catalyst used for 890 h in the rig, and for the catalyst used for 2299 h.

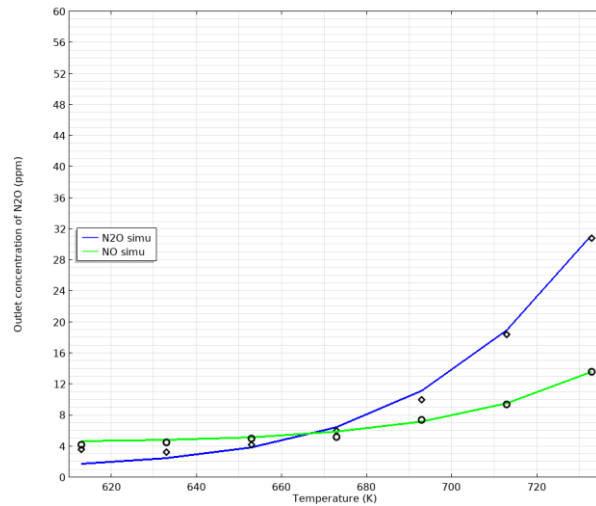
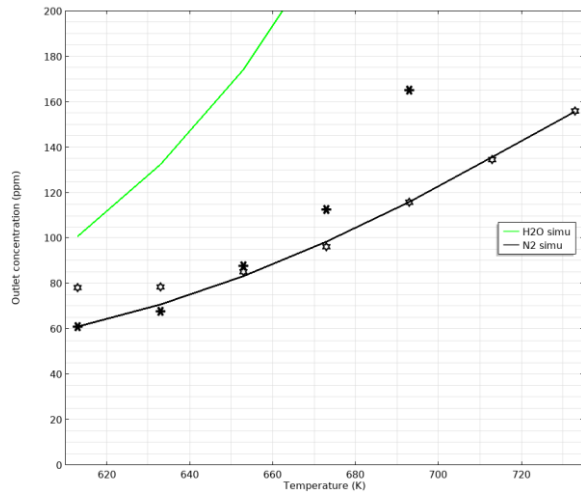
For the fresh catalyst, the fit to N<sub>2</sub> is not very good at low and high temperatures. The experimental values show a curved upward deviation from the simulated ones for the fresh catalyst and the one used for 890 h. The best fit for N<sub>2</sub> is obtained on the catalysts used for 2299 h. The SCR is also active at high temperatures where we know that small amounts of NO are formed from NH<sub>3</sub>. So, the high experimental values at temperatures above 700 K values can be explained if the SCR reaction takes place to a small extent. Figure 8 shows that it is quite easy to get a good fit for the contents of N<sub>2</sub>, N<sub>2</sub>O, and NO except for the lowest temperatures.

The simulated concentration of H<sub>2</sub>O is shown in Fig 8 and are also much higher than the experimental ones but with an increased discrepancy at increased temperatures. Also, the experimental value of H<sub>2</sub>O is lower for the catalyst used for 2299 h than for the other ones. Whether this is significant is hard to say.

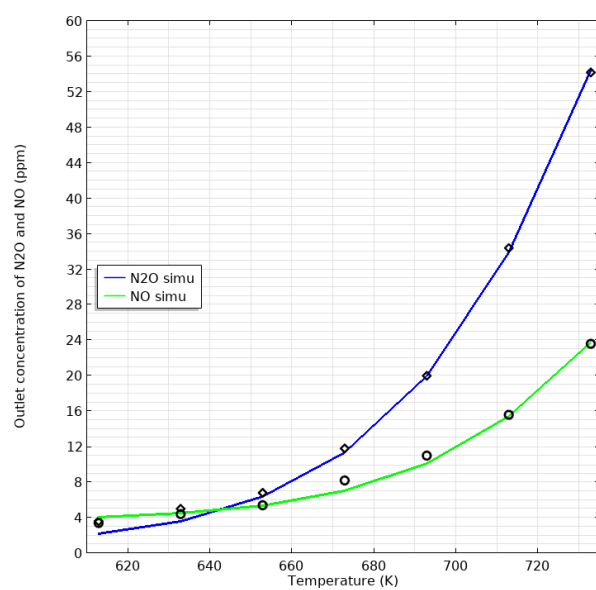
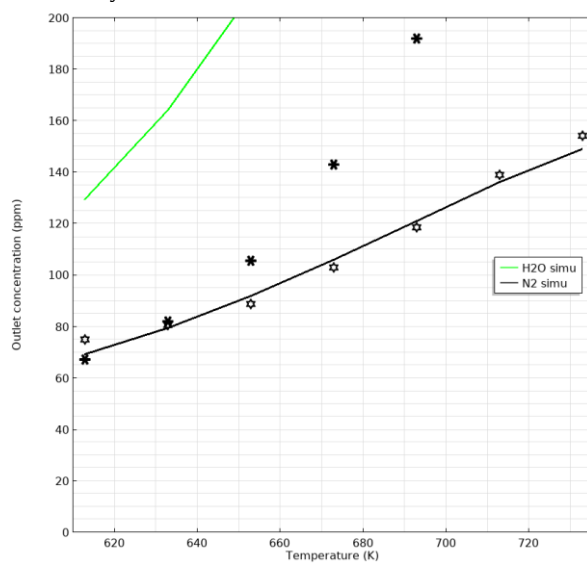
Fig 9 shows the simulated and experimental values of NH<sub>3</sub> when the fitting is performed on the formation of N<sub>2</sub>. The best fit is obtained at an intermediate temperature.

At 733 K, the experimental value is 300 ppm, while the simulated one is 400 ppm. All components are measured precisely as before [11], so some effects of the deactivation could explain the not too good fit for H<sub>2</sub>O (Fig 8) and NH<sub>3</sub> (Fig 9). A plausible one is that Ca phosphates are present on the deactivated catalysts reacting with and consuming the gas-phase water [17]. This reaction will not give a long-lasting effect, in any case. Furthermore, it will not explain that similar behaviour is observed for the fresh catalyst. A fact is that the mass balance in these experiments is not as correct as in earlier work [11]. The discrepancy increases at increased temperatures. For N<sub>out</sub>/N<sub>in</sub> the mean is 0.962±0.034, and for H<sub>out</sub>/H<sub>in</sub> it is 0.847±0.074. Values at the lowest temperature are close to 1. For the earlier study, the standard deviation was only 0.9 % and independent on temperature. Thus, the use of N<sub>2</sub> instead of NH<sub>3</sub> for the fitting procedure.

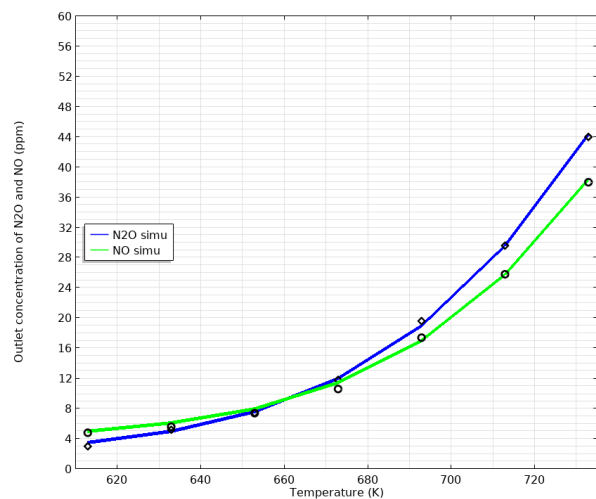
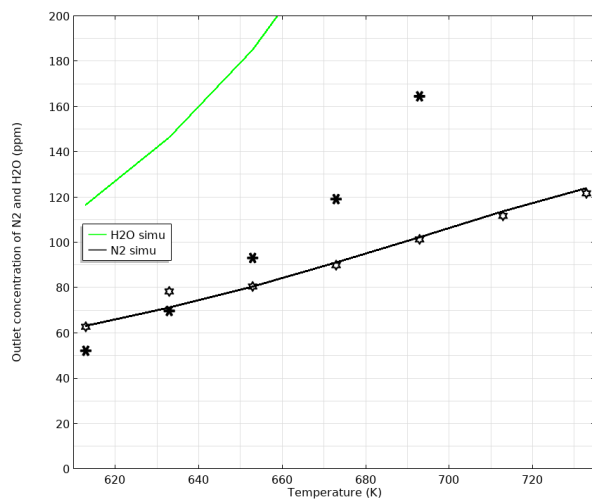
Table 5 shows the obtained kinetic parameters after fitting the simulated concentrations of N<sub>2</sub>, N<sub>2</sub>O, and NO to the experimental ones at increasing temperatures for the three catalysts studied.



Fresh catalyst



The catalyst used for 890 h



The catalyst used for 2299 h

**Fig 8.** Simulation of the oxidation of about 700 ppm NH<sub>3</sub> with 2 % O<sub>2</sub> at 1.24 bar over the fresh catalyst and the ones used for 890 and 2299 h. Experimental values for N<sub>2</sub> (stars), H<sub>2</sub>O (asterisks), N<sub>2</sub>O (diamonds), and NO (circles). Lines are simulated values

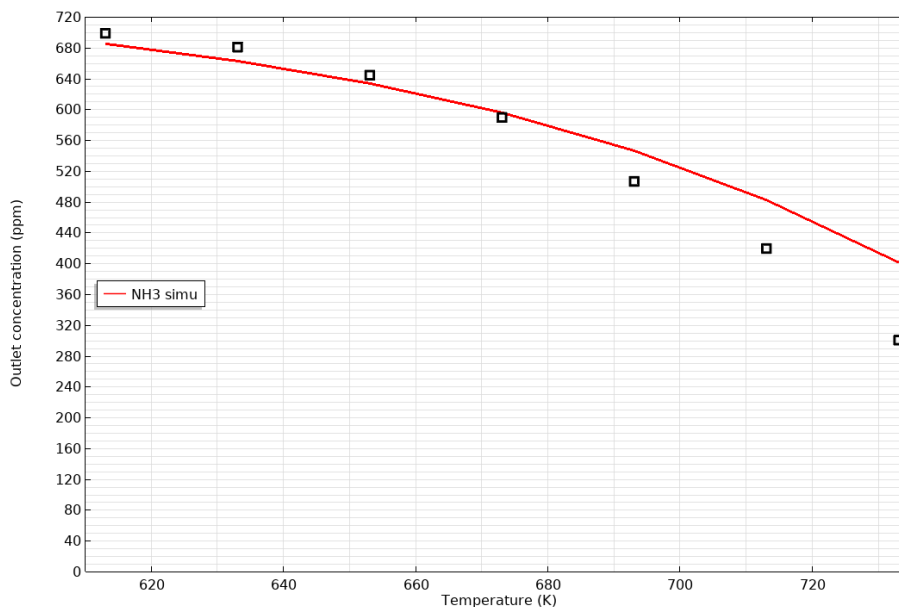


**Fig 9.** Outlet concentration of NH<sub>3</sub> as a function of temperature for the fresh catalyst. oxidation of 745.6 ppm NH<sub>3</sub> in 2 % O<sub>2</sub> on the fresh catalyst. Squares are experimental values while the line is the simulated ones

**Table 5.** Simulated kinetic parameters in the oxidation of 700 ppm NH<sub>3</sub> with 2 % O<sub>2</sub> in Helium at 1.236 bar from 340 to 460 °C as a function of time of use for the three catalysts studied. Rates are given at inlet conditions

Parameter	Fresh	890 h	2299 h
A <sub>2</sub> (s <sup>-1</sup> )	1.51*10 <sup>6</sup>	3.93*10 <sup>5</sup>	1.62*10 <sup>5</sup>
E <sub>2</sub> (kJ mol <sup>-1</sup> )	64	56	52
r <sub>2</sub> (mol m <sup>-3</sup> s <sup>-1</sup> )	9.3*10 <sup>-2</sup> - 5.9*10 <sup>-1</sup>	1.3*10 <sup>-1</sup> - 5.8*10 <sup>-1</sup>	1.0*10 <sup>-1</sup> - 4.2*10 <sup>-1</sup>
A <sub>4</sub> (s <sup>-1</sup> )	7.17*10 <sup>10</sup>	5.78*10 <sup>10</sup>	4.01*10 <sup>9</sup>
E <sub>4</sub> (kJ mol <sup>-1</sup> )	138	133	118
r <sub>4</sub> (mol m <sup>-3</sup> s <sup>-1</sup> )	2.2*10 <sup>-3</sup> - 1.5*10 <sup>-1</sup>	3.1*10 <sup>-3</sup> - 2.6*10 <sup>-1</sup>	6.0*10 <sup>-3</sup> - 2.1*10 <sup>-1</sup>
A <sub>5</sub> (s <sup>-1</sup> )	1.25*10 <sup>11</sup>	9.12*10 <sup>10</sup>	4.36*10 <sup>9</sup>
E <sub>5</sub> (kJ mol <sup>-1</sup> )	153	146	124
r <sub>5</sub> (mol m <sup>-3</sup> s <sup>-1</sup> )	2.4*10 <sup>-4</sup> - 2.2*10 <sup>-2</sup>	5.8*10 <sup>-4</sup> - 4.2*10 <sup>-2</sup>	2.0*10 <sup>-3</sup> - 8.4*10 <sup>-2</sup>

The formation rates of N<sub>2</sub>, obtained in the simulations, as shown in Table 5, increase at 340 °C for the catalyst used for 890 h compared to the fresh catalyst but decrease on further use. At 460 °C it decreases by 2 % after 890 h and decreases by 29 % after 2299 h compared to the fresh catalyst. Earlier results, where an increased content of sulphur increases the rate of reaction in the SCR, especially at low temperatures [15,16] agrees with this finding. At 340 °C the rates of formation of N<sub>2</sub>O (r<sub>4</sub>) increase by 41 % after 890 h and increase by 273 % after 2299 h from the value for the fresh catalyst. At 460 °C the rate increase after 890 h by 73 % and by 40 % after 2299 h. The lowest rate of formation of NO at 340 °C is observed on the fresh catalyst increasing by 242 % after 890 h and by a 833 % after 2299 h. At higher temperatures, the effects are smaller but except for the catalyst used for 2299 h where an increase by 382 % is observed.

The activation energies for the formation of N<sub>2</sub>, N<sub>2</sub>O, and NO all decrease when the catalyst is poisoned. The same effect has been observed before [11]. A decrease

in the pre-exponential factor, proportional to the number of active sites, is also observed.

Efstathiou and Fliatoura [8] determined the apparent activation energy of 61.4 kJ mol<sup>-1</sup> for the oxidation of 1000 ppm NH<sub>3</sub> with 2 % O<sub>2</sub> in Helium for an 8 % V<sub>2</sub>O<sub>5</sub>/TiO<sub>2</sub> catalyst from experimental rates. The rate of N<sub>2</sub> formation at 300 °C was 17.2\*10<sup>-6</sup> mol g<sup>-1</sup> min<sup>-1</sup> compared to the value in this study of 9.3\*10<sup>-2</sup> mol m<sup>-3</sup> s<sup>-1</sup> (2.4\*10<sup>-6</sup> mol g<sup>-1</sup> min<sup>-1</sup>) at 340 °C. Their E<sub>2</sub> was 61.4 kJ mol<sup>-1</sup> compared to the value in this study of 64 kJ mol<sup>-1</sup>. The experimental rate data of Efstathiou and Fliatoura [8] were obtained on the powdered catalyst, but the particle size is not mentioned, so an estimation of diffusion influence is not possible. Taking into consideration that the data from this study are obtained on a layered monolithic catalyst, the activities are similar.

If we assume that, the reaction rate of reaction 2 is the same under SCR conditions as under NH<sub>3</sub> oxidation conditions, we can compare the values of Salehi et al. [18] to ours. They also simulated a monolithic

structure with a catalyst layer. Their values of the pre-exponential factor and the activation energy for the formation of  $N_2$  were  $6.8 \cdot 10^7$  and 85 compared to the values of this study of  $1.51 \cdot 10^6$  and 64  $\text{kJ mol}^{-1}$ , respectively. Salehi et al. [18] also used first order in ammonia concentration for the rate of formation of  $N_2$ . A calculation of the rate  $r_2$  at 340 °C from their data gives  $0.256 \text{ mol m}^{-3} \text{ s}^{-1}$  compared to the value from this study of  $9.3 \cdot 10^{-2} \text{ mol m}^{-3} \text{ s}^{-1}$  (Table 5). They are in the same magnitude.

Om et al. [19] studied, using Fluent, the SCR in a monolith isothermally. The concentrations of NO and  $NH_3$  were in the range of 1000 ppm, so we believe that their simulation should have been non-isothermal for more precise results. Schaub's data [20] were taken from an experimental study on a catalytic filter consisting of very small catalyst particles, so the values should be close to intrinsic values. Their values of  $k_2$  and  $E_2$  were  $6.73 \cdot 10^7$  and  $85.4 \text{ kJ mol}^{-1}$  while the values of this study were  $1.51 \cdot 10^6$  and 64  $\text{kJ mol}^{-1}$ , respectively (Table 5). Calculation of nitrogen formation rates at 340 °C from the data of Om et al. [19] gave a value of 0.049 while the value in this study was  $0.093 \text{ mol m}^{-3} \text{ s}^{-1}$ . The rates are in the same range at this temperature. At 460 °C, their rate was 4.8, and the value of this study was  $0.59 \text{ mol m}^{-3} \text{ s}^{-1}$ .

Chen and Tan [13] simulated a catalytic particle bed for the SCR process. In their simulation, the rate constant for the formation of  $N_2$  from  $NH_3$  by oxidation ( $k_2$ ) was  $6.73 \cdot 10^7 \cdot \exp(-84400/R/T)$ . This study's result was a rate constant expression of  $1.51 \cdot 10^6 \cdot \exp(-64000/R/T)$ . Thus, at 460 °C the rate constants are 65 and 42  $\text{s}^{-1}$  respectively, which is again in the same range.

Millo et al. [22] simulated the SCR on a filter catalyst for automotive applications. Besides the standard SCR, the fast and slow SCR, the oxidation of  $NH_3$  to  $N_2$  was used as model reactions. The activation energy ( $E_2$ ) was  $144.6 \text{ kJ mol}^{-1}$  again much higher than this study's value of  $57 \text{ kJ mol}^{-1}$ . Their rate expression was  $r_2 = k_2 \cdot C_{NH_3} \cdot C_{O_2}$  and includes the dependence on the oxygen concentration making direct comparisons unsuitable. Their experiments also included water which would decrease the rate of all reactions.

#### 4. CONCLUSIONS

In this study the of oxidation of ammonia with  $O_2$  was simulated using COMSOL Multiphysics showing the three products  $N_2$ ,  $N_2O$  and NO appearing at increasing temperatures. All reactions were of the first order in the concentration of  $NH_3$ . Apparent data show strong effects of the deactivation on the kinetics. The apparent activation energies decrease when the catalyst gets deactivated. The effects of the rate of formation of  $N_2$  by poisoning is minimal if any. Both the formation of  $N_2O$  and NO show decreased activation energies when the catalysts are deactivated. Their pre-exponential factors decrease considerably too. All products of the oxidation of  $NH_3$  with  $O_2$  could be nicely represented in the simulation when the concentrations of  $N_2$ ,  $N_2O$ , and NO were fitted. The concentrations of  $NH_3$  and  $H_2O$  obtained by a mass balance in the simulation were not close to experimental values.

#### ACKNOWLEDGEMENTS

The author wishes to thank Mr Martin Bruszt, who performed the reaction experiments. A Swedish diesel engine test company is acknowledged for supplying the fresh and deactivated catalyst samples as well as the testing unit. This simulation study did not receive any specific grants from funding agencies in the public, commercial, or not-for-profit sectors.

#### REFERENCES

- [1]. A. Konstandopoulos, D. Zarvalis, L. Chasapidis, L. Deloglou, N. Vlachos, A. Kotbra, and G. Anderson, "Investigation of SCR Catalysts for Marine Diesel Applications", *SAE International Journal of Engines*, Vol. 10 (4), pp. 1653-1666, 2017.
- [2]. H. Jung, D.B. Kittelson, and M.R. Zachariah, "The Influence of Engine Lubricating Oil on Diesel Nanoparticle Emissions and Kinetics of Oxidation", *SAE Technical Paper*, 2003-01-3179, 2003.
- [3]. C.U.I. Odenbrand, "Penetration of Poisons Along the Monolith Length of a  $V_2O_5/TiO_2$  Diesel SCR Catalyst and Its Effect on Activity", *Catalysis Letters*, Vol. 149(12), pp. 3476-3490, 2019.
- [4]. M. Koebel, and M. Elsener, "Selective catalytic reduction of NO over commercial DeNOx-catalysts: experimental determination of kinetics and thermodynamic parameters", *Chemical Engineering Science*, Vol. 53 (4), pp. 657-669, 1998.
- [5]. U.S. Ozkan, Y. Cai, M.W. Kuthekar, and L. Zhang, "Role of Ammonia Oxidation in Selective Catalytic Reduction of Nitric Oxide over Vanadia Catalysts", *Journal of Catalysis*, Vol. 142, pp.182-197, 1993.
- [6]. U.S. Ozkan, Y. Cai, and M.W. Kuthekar, "Investigation of the Mechanism of Ammonia Oxidation and Oxygen Exchange over Vanadia Catalysts Using N-15 and O-18 Tracer Studies", *Journal of Catalysis*, Vol. 149, pp.375-389, 1994.
- [7]. B.L. Duffy, H.E. Curry-Hyde, N.W. Cant, and P.F. Nelson, "Isotopic Labelling Studies of the Effects of Temperature, Water and Vanadia Loading on the Selective Catalytic Reduction of NO with  $NH_3$  over Vanadia-Titania Catalysts", *Journal of Physical Chemistry*, Vol. 98, pp. 7153-7161, 1994.
- [8]. A.M. Efstathiou, and K. Fliatoura, "Selective catalytic reduction of nitric oxide with ammonia over  $V_2O_5/TiO_2$  catalyst; A steady-state and transient kinetic study", *Applied Catalysis B: Environmental*, Vol. 6, pp. 35-59, 1995.
- [9]. S. Djerad, M. Crocoll, S. Kureti, L. Tifouti, and W. Weisweler, "Effect of oxygen concentration on the  $NO_x$  reduction with ammonia over  $V_2O_5-WO_3/TiO_2$  catalyst", *Catalysis Today*, Vol. 113, pp. 208-214, 2006.
- [10]. C.U.I. Odenbrand, "High Temperature and High Concentration SCR of NO with  $NH_3$  for the Oxyfuel Combustion Process: Fitting of Kinetics to Data from a Laboratory Reactor Experiment", *Topics in Catalysis*, Vol. 60, pp. 1317-1332, 2017

- [11]. C.U.I. Odenbrand, "CaSO<sub>4</sub> deactivated V<sub>2</sub>O<sub>5</sub>-WO<sub>3</sub>/TiO<sub>2</sub> SCR catalyst for a diesel power plant. Characterization and simulation of the kinetics of the SCR reactions", *Applied Catalysis B: Environmental*, Vol. 234, pp. 365-377, 2018.
- [12]. B. Roduit, A. Wokaun, and A. Baiker, "Global Kinetic Modeling of Reactions Occurring during Selective Catalytic Reduction of NO by NH<sub>3</sub> over Vanadia/Titania-Based Catalysts", *Industrial & Engineering Chemistry Research*, Vol. 37, pp. 4577-4590, 1998.
- [13]. C.-T. Chen, and W.-L. Tan, "Mathematical modeling, optimal design and control of an SCR reactor for NO<sub>x</sub> removal", *J. of the Taiwan Institute of Chemical Engineers*, Vol. 43, pp.409-419, 2012.
- [14]. [http://www.engineersedge.com/heat\\_transfer/convective\\_heat\\_transfer\\_coefficients\\_13378](http://www.engineersedge.com/heat_transfer/convective_heat_transfer_coefficients_13378).
- [15]. J.G.M.Brandin, and C.U.I. Odenbrand, "Poisoning of SCR Catalysts used in Municipal Waste Incineration Applications", *Topics in Catalysis*, Vol. 60, pp. 1306-1316, 2017.
- [16]. J.G.M.Brandin, and C.U.I. Odenbrand, "Deactivation and Characterization of SCR Catalysts Used in Municipal Waste Incineration Applications", *Catalysis Letters*, Vol. 148 (1), pp. 312-327, 2018.
- [17]. T.C. Vaimakis, P.J. Pomonis, and A.T. Sdoukos, "A detailed study of the condensation of the Ca(H<sub>2</sub>PO<sub>4</sub>)<sub>2</sub>\*H<sub>2</sub>O-CaHPO<sub>4</sub>\*2H<sub>2</sub>O system under thermal treatment", *Thermochimica Acta*, Vol. 168, pp.103-113, 1990.
- [18]. S. Salehi, M.A. Moghaddam, and N. Sahebamee, "Modeling Transport Phenomena in Selective Catalytic Reductant Catalytic Converter with NH<sub>3</sub> as reductant for NO Degradation", *International Journal of Engineering*, Vol. 29 (9), pp. 1183-1190, 2016.
- [19]. J. Om, P. Ji, and W. Wu, "3D Numerical Simulation of Gas Flow and Selective Catalytic Reduction (SCR) of NO in the Honeycomb Reactor", *Asia-Pacific Energy Equipment Engineering Research Conference (AP3ER 2015)*, pp. 56-59, Atlantis Press, 2015.
- [20]. G. Schaub, D. Unruh, J. Wang, and T. Turek, "Kinetic analysis of selective catalytic NO<sub>x</sub> reduction (SCR) in a catalytic filter", *Chemical Engineering and Processing*, Vol. 42, pp. 365-371, 2003.
- [21]. F. Millo, M. Rafigh, D. Fino, and P. Micelli, "Application of a global kinetic model on an SCR coated on Filter (SCR-F) catalyst for automotive applications", *Fuel*, Vol. 198, pp. 183-192, 2017.